Proceedings of the Seventh International Conference on
Railway Technology: Research, Development and Maintenance
Edited by: J. Pombo
Civil-Comp Conferences, Volume 15, Paper 9.2
Civil-Comp Press, Edinburgh, United Kingdom, 2026
ISSN: 2753-3239, doi: 10.4203/ccc.15.9.2

Evaluation for Braking Performance and Mechanical Properties of Alloy Cast Iron Brake Blocks with Slits

K. Ikeuchi and K. Handa

Railway Technical Research Institute, Japan

Abstract

This study investigates the braking performance and stress characteristics of cast iron brake blocks featuring different slit configurations, developed for electric and diesel multiple units operating in cold and snowy regions. Bench tests were conducted using two brake block types – Type A with conventional slit geometry and Type B with alternating non-through slits – to evaluate friction coefficient, braking distance, wear behaviour, and stress distribution. Normal operation brake tests showed minimal performance differences between the two types, while emergency brake tests demonstrated that Type B achieved approximately 10% shorter braking distances at high speeds. Type B exhibited slightly greater wear, attributed to its larger slit area and reduced apparent contact area. Stress measurements using strain gauges revealed that, although Type B experienced higher tensile stress at the slit bottom during wheel stoppage, the stresses acting directly on the slit area during braking were reduced by nearly 70% compared with Type A. Finite-element analysis further supported the experimental trends, confirming stress concentration at slit bottoms and overall consistency with measured values. These results suggest that the alternating slit design of Type B offers equal or superior braking performance while effectively reducing maximum stresses acting on the brake block.

Keywords: brake block, cast iron, brake test, braking performance, mechanical property, finite element analysis.

1 Introduction

Alloy cast iron brake blocks are widely used on electric multiple units (EMU) and diesel multiple units (DMU) in Japan's Hokkaido region due to their stable performance in low temperatures and snowfall. With the increasing speeds of EMU and DMU, efforts to enhance the braking performance of cast iron brake blocks have been made through measures such as adding alloying elements, trialling ceramic foams, and adding slits.[1][2][3]

Focusing on the addition of slits, while these stabilise and increase the contact area with the wheel, thereby improving the friction coefficient, concerns exist regarding the strength of the slit sections. Consequently, modifications to the slit design have been implemented. Among these, a configuration featuring non-through slits arranged in an alternating pattern is considered advantageous for strength, as the slits do not penetrate the widthwise direction. The shape is shown in Figure 1.[4]

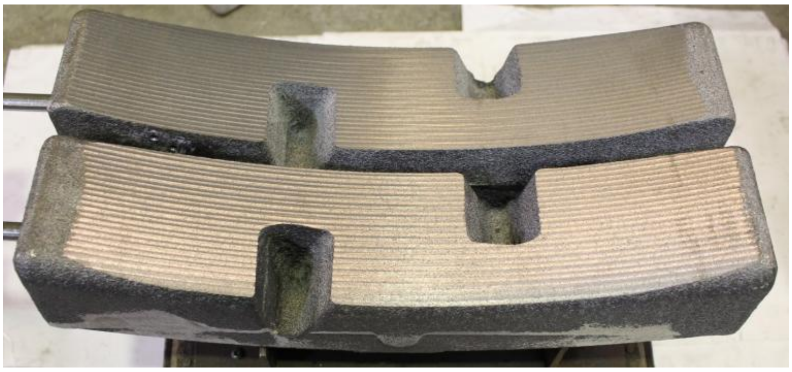

Figure 1: Alloyed cast iron brake blocks with non-through slits

However, there are no previous examples evaluating the stresses on these slits alongside the brake performance of the brake block body itself. From a quality assurance perspective, verification has been limited to confirming strength using material testing machines, etc.

Therefore, we conducted bench tests on cast iron brake blocks with slits to confirm their braking performance. We also measured the stresses occurring near the brake block slits during braking and estimated these stresses using numerical calculations.

2 Investigation of Brake Performance through Bench Test

2.1 Methods

Bench tests were conducted on the Railway Technical Research Institute's brake testing machine to verify fundamental brake block performance, such as friction coefficient and braking distance. The testing machine is shown in Figure 2. To simulate a vehicle where two brake blocks act on one wheel, identical brake blocks were installed on both sides of the wheel for the experiment. Other test conditions are shown in Table 1.

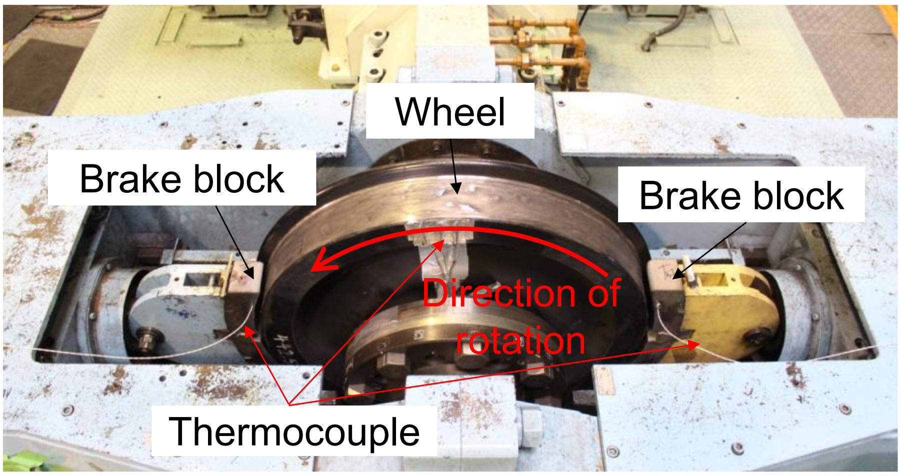

Figure 2: Testing machine

Wheel	JIS E5402-1 SSW-QS B type Diameter: 810 mm	
Brake block	Alloyed cast iron brake block Principal alloying element: P, Mo, Cr	
Flywheel inertia	1066 kg・m²	
Braking condition	Speed	Braking force
Normal operation brake condition	30 km/h	8 kN
	50 km/h	15 kN
	65 km/h	15 kN
Emergency brake condition	35 km/h	25 kN
	65 km/h	25 kN
	95 km/h	25 kN
	125 km/h	40 kN
	135 km/h	40 kN

Table 1: Testing condition

The brake blocks were Type A, designed for express DMU and EMU in Hokkaido, and Type B, featuring a different slit configuration. The alloy composition was identical for both types.

The tests commenced with preliminary trials to conform the friction surfaces of the brake blocks to the wheel profile, followed by various brake tests. The normal operation brake test simulated the brake application force frequently used during normal operation, while the emergency brake test simulated the force applied during emergency stops.

Brake block performance was evaluated based on braking distance, friction coefficient, wear thickness calculated from the friction surface shown in Figure 3, and weight reduction.

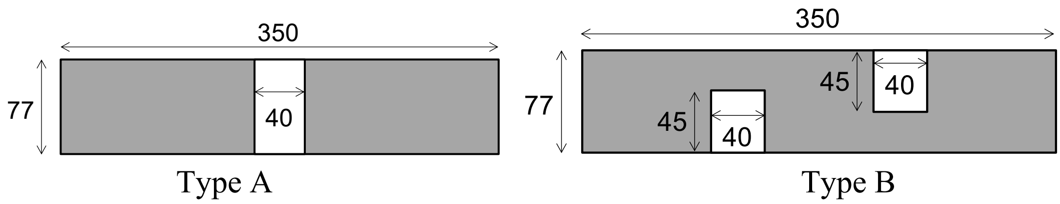

Figure 3: Friction surface of brake blocks

2.2 Results

The friction coefficients obtained from the normal operation brake tests are shown in Figure 4. Figure 5 shows the average braking distances, and Figure 6 shows the average wear thicknesses. Under all test conditions, there was no significant difference between Type A and Type B. Type B tended to have shorter braking distances and higher deceleration. The wear thickness was slightly greater for Type B.

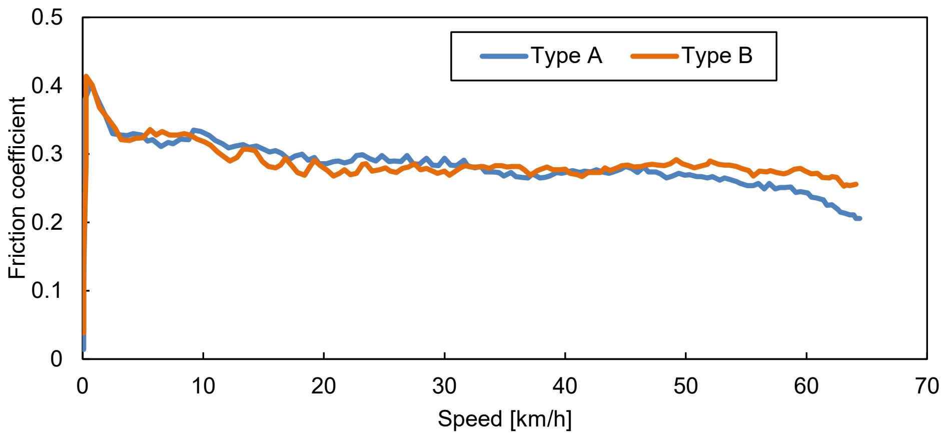

Figure 4: Friction coefficients in experiment. (65 km/h, 15 kN)

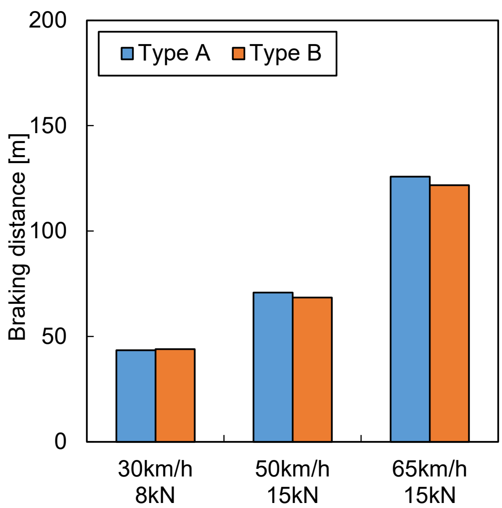

Figure 5: Average of braking distance.

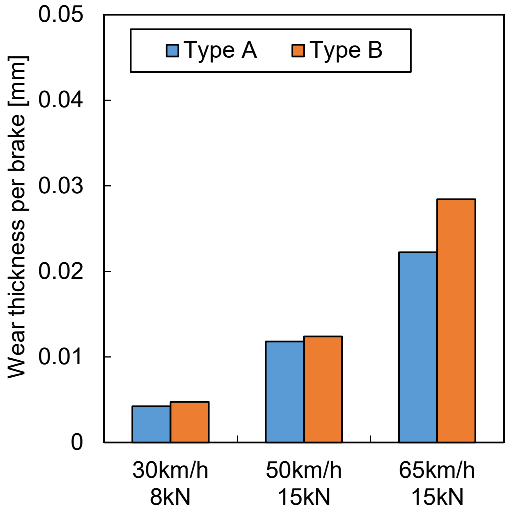

Figure 6: Average of wear thickness of brake block.

Figure 7 shows the change in the friction coefficient during the emergency brake test. Figure 8 shows the average braking distance, and Figure 9 shows the average wear thickness. Compared to Type A, Type B exhibited a shorter braking distance, particularly in high-speed tests, achieving a reduction of approximately 10%. Wear thickness was slightly greater for Type A at low speeds and for Type B at high speeds. Furthermore, there was little difference in brake block temperature, with the maximum reaching approximately 500 °C.

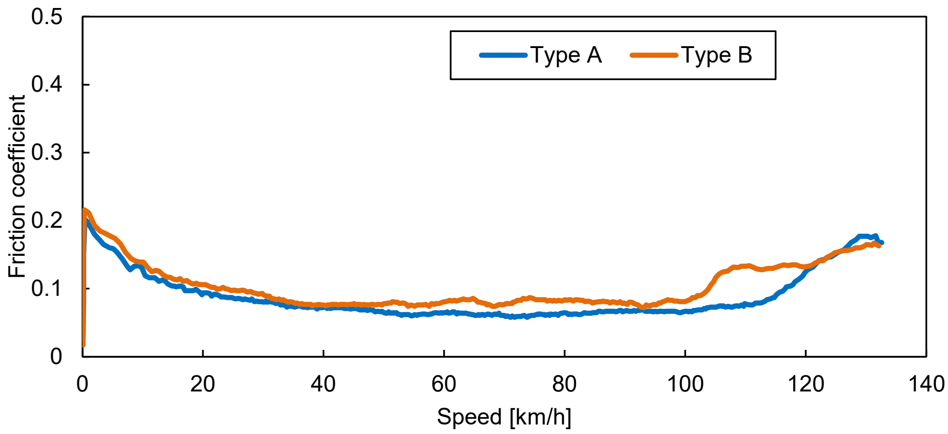

Figure 7: Friction coefficients in experiment. (135 km/h, 40 kN)

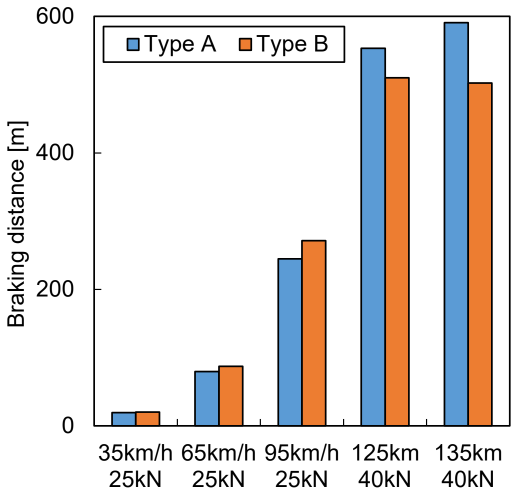

Figure 8: Average of braking distance.

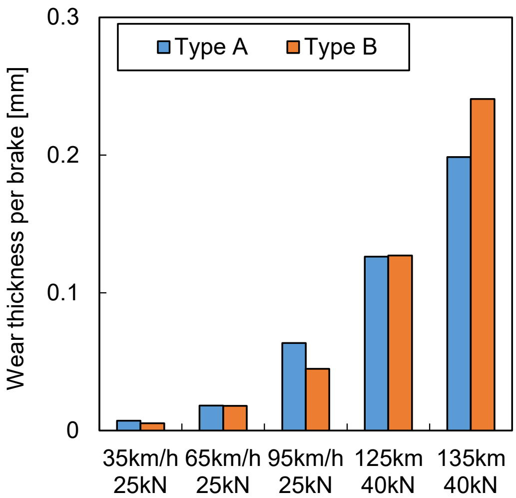

Figure 9: Average of wear thickness of brake block.

3 Stress Measurement Test

3.1 Methods

To measure stresses occurring near the brake block slit section, separate from the brake performance verification tests described in the preceding sections, a bench brake test was conducted with strain gauges affixed to the brake block.

Test conditions were identical to those in Table 1. Additionally, tests were conducted where the brake block was pressed against the wheel during wheel stoppage to measure tensile strain. Loads applied were 8 kN, 15 kN, 25 kN, and 40 kN.

Strain gauges for stress measurement, as shown in Figures 10 and 11, were affixed to the brake blocks for use in the experiments. Strain gauges suitable for mild steel were used. They were bonded with adhesive to a surface smoothed by a grinder and then cured with an epoxy-based adhesive.

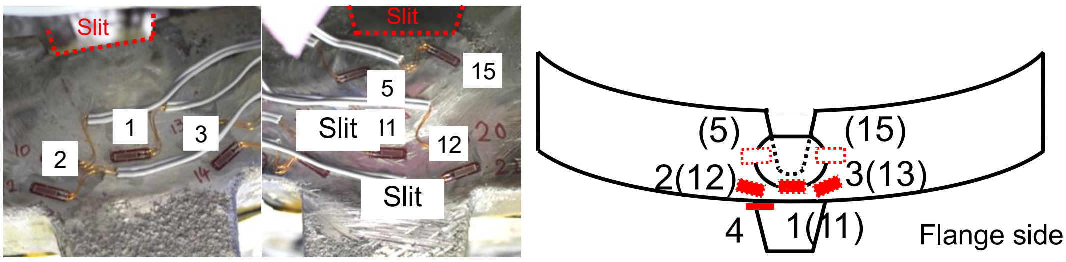

Figure 10: Position of strain gauges in Type A.
(Dotted lines and bracketed numbers indicate the reverse side of the paper.)

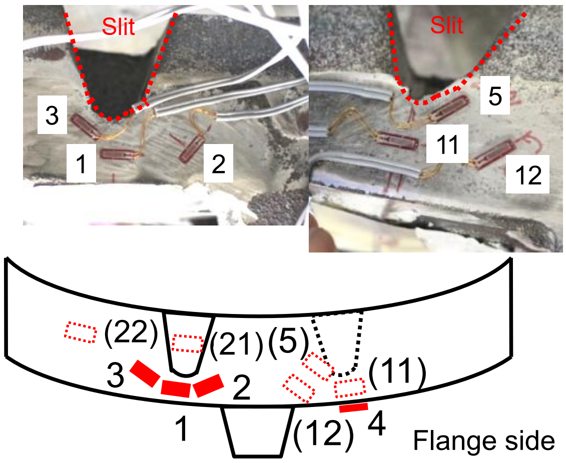

Figure 11: Position of strain gauges in Type B.
(Dotted lines and bracketed numbers indicate the reverse side of the paper.)

3.2 Results

The results of the wheel stopping test are shown in Figure 12. These results were obtained when the brake block was pressed against the wheel at 8 kN, representing the average of measurements taken while the brake pressure was applied. Note the presence of tensile stress acting in the direction of opening the slit or crack. In Type A, tensile stress was generally present at locations such as No. 5, which corresponds to the slit entrance, and No. 4 on the rear face. In Type B, tensile stress was present at locations No. 3, 5, 11, and No. 22, which are closer to the bottom of the slit section. Although the absolute values of tensile stress were larger in Type B, they are not considered to be at a level that would adversely affect the slit.

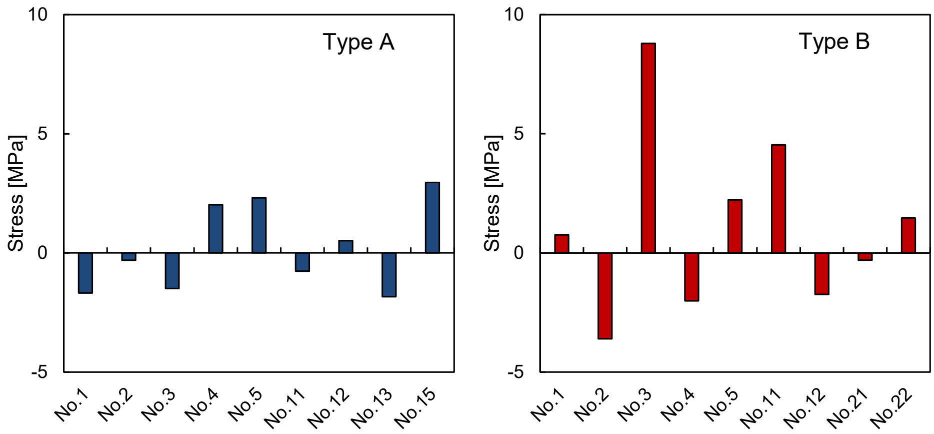

Figure 12: Result of static stress in brake block.

Examples of results from the dynamic stress measurement tests are shown in Figures 13 and 14. As stress varies with speed, depending on the location of the strain gauge, the stress transitioned from tensile to compressive stress at certain points during braking. In this test, while the tensile stress for Type A was primarily at No.5 and No.15 near the slit section, the tensile stress for Type B mainly acted at No. 21 and No. 22, which are not in the slit section.

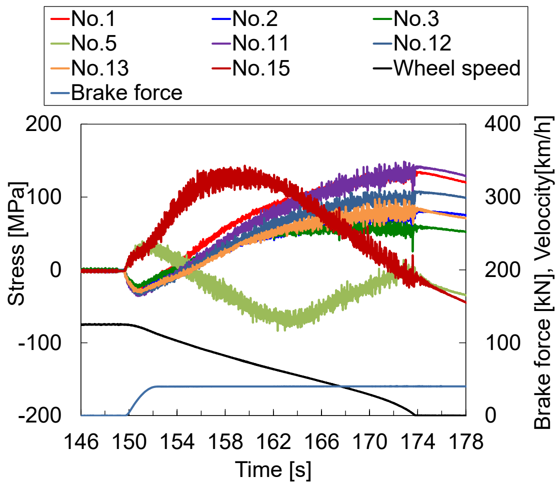

Figure 13: Relationship between dynamic stress, brake force and wheel speed. (Type A)

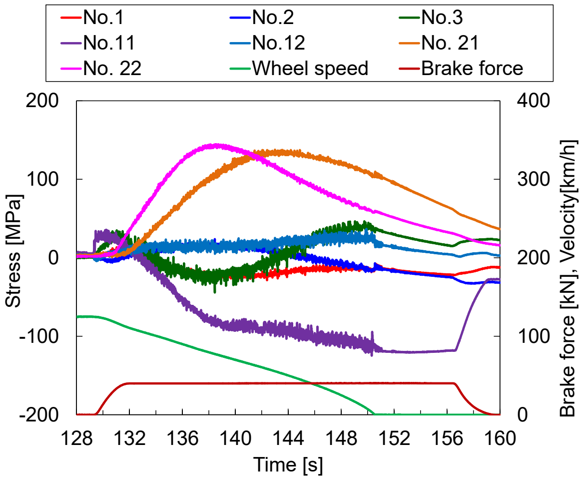

Figure 14: Relationship between dynamic stress, brake force and wheel speed. (Type B)

Due to significant vibration during brake operation, the results were evaluated using the maximum tensile stress value recorded at the strain gauge closest to the slit section during braking. The outcome is shown in Figure 15. Across all speed ranges, the maximum stress value was lower for Type B. Notably, the stress value at gauge 2 (between the slit bottom and the brake block mounting section) was reduced by approximately 70%.

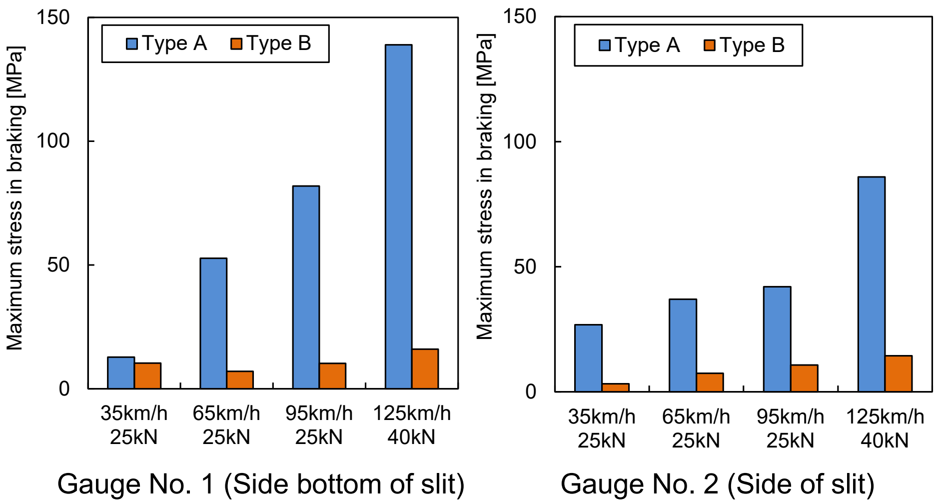

Figure 15: Maximum stress in braking test.

4 Stress Analysis of Cast Iron Brake Blocks

4.1 Modelling methods

To estimate the stress distribution across the entire brake block, including areas where strain gauges could not be applied, such as near the friction surface and within the material, a three-dimensional numerical analysis modelling the wheel and brake block was conducted based on the experiments in the previous section.

The brake block model is shown in Figure 16. The brake block was modelled as a uniform elastic body. The applied load distribution (equivalent to 8 kN braking force) was applied to the area where the brake block support contacts the rear surface. The friction surface side was modelled as contacting a rigid wheel with the designed shape. Material properties were set as Young's modulus 200 GPa and Poisson's ratio 0.27, equivalent to grey cast iron. Under these conditions, a static analysis was performed using the finite element method. NASTRAN was used as analysis software. The mesh size near the slit is smaller than in other areas.

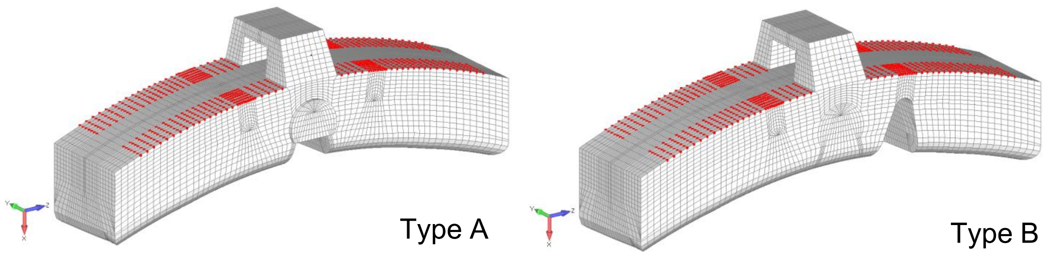

Figure 16: Model of brake block.

4.2 Results

Figures 17 and 18 show the stress distribution occurring in the circumferential direction of the brake block when the braking force is applied. The shades in the figures indicate the magnitude of the stress. The locations indicated by solid black arrows in the figures are near points where stresses were experimentally measured; the measured values are those obtained in the previous section. At these locations, the trends in tensile stresses were generally consistent, irrespective of the measured and analysed values. However, some locations showed slight discrepancies between measured and analysed values. This is thought to be due to the brake block and wheel shapes used in the experiments differing from the design shape as the tests progressed.

The locations indicated by black dashed arrows in the figures are near points where the maximum tensile stress was obtained from the analysis. Analysis revealed that the maximum stress occurred at the inner bottom of the slit, with Type B exhibiting higher stress than Type A. These locations could not be measured in the result of Figure 12; the maximum tensile stress measured in the vicinity of the slit was higher for Type B than for Type A, suggesting a similar trend.

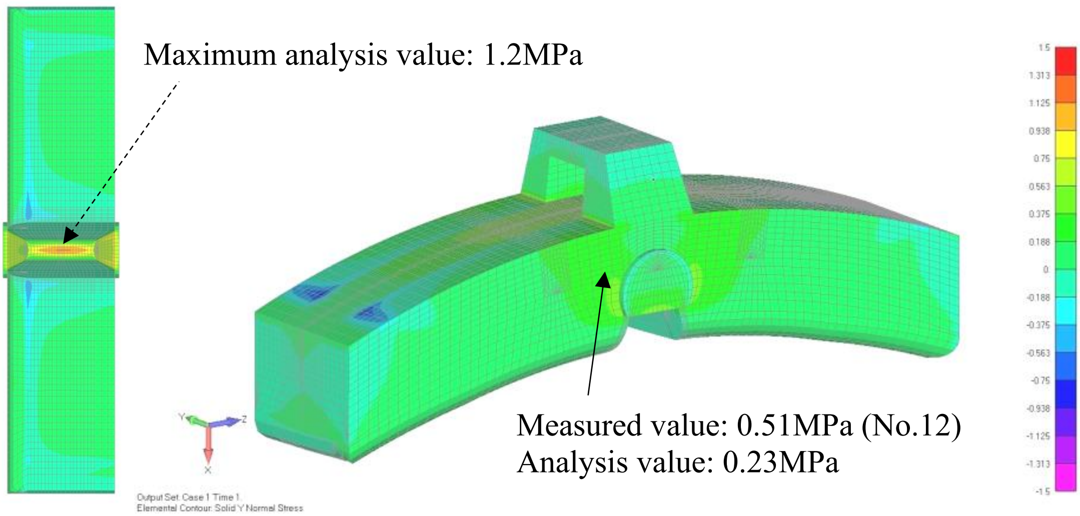

Figure 17: Result of analysis for stress distribution in Type A brake block.

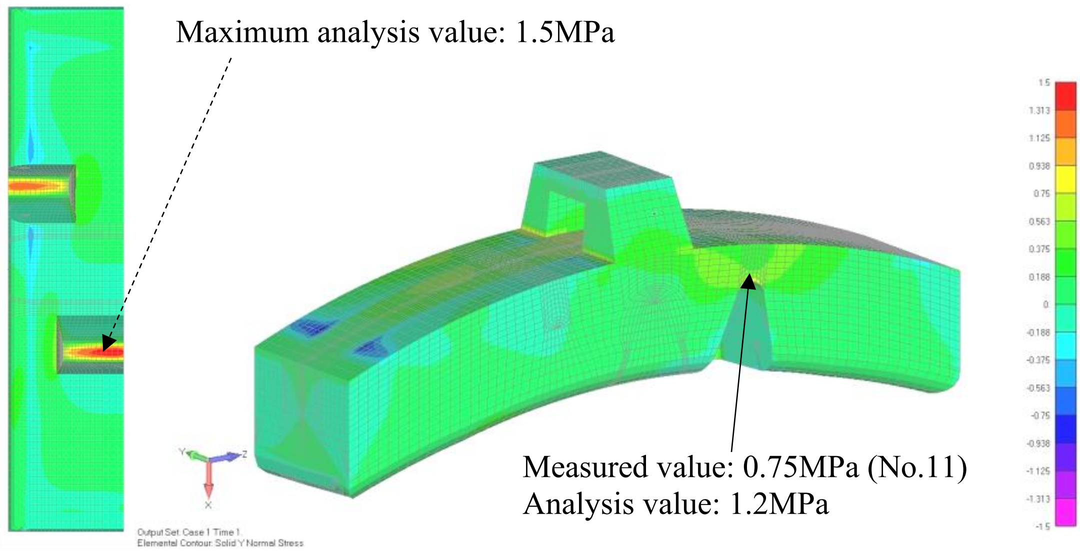

Figure 18: Result of analysis for stress distribution in Type B brake block.

5 Conclusions and Contributions

Two distinct brake block designs featuring different slit shapes, developed to enhance the speed of conventional railway vehicles using cast iron brake blocks, underwent various performance evaluations on a bench tread brake testing machine. Simultaneously, stresses acting near the slits during braking were measured and analysed using similar methodologies. The results are as follows.

Regarding brake performance evaluation via tread brake testing, while little difference was observed between Type A and Type B during normal operation braking, emergency braking tests revealed that Type B achieved approximately 10% shorter braking distances than Type A at high speeds. However, Type B exhibited slightly higher wear rates, attributed to its smaller apparent contact area and larger actual worn area compared to Type A.

Using the same test apparatus and brake blocks fitted with strain gauges on the slotted sections, stresses occurring near the slotted areas were measured. The results showed that during wheel stoppage, the stress of the slotted area of Type B was larger than that of Type A. Furthermore, during wheel rotation, unlike when stationary, both tensile and compressive stresses acted depending on the speed range. Focusing specifically on the slit section, Type B achieved a reduction in stresses occurring there of nearly 70% compared to Type A.

Numerical analysis was also conducted to verify the stresses within the brake blocks during wheel stoppage. The results indicated that, irrespective of brake block shape, Type B tended to exhibit higher maximum tensile stresses than Type A.

Based on these results, it is conceivable that Type B, with staggered slits, possesses performance equivalent to or superior to Type A with centrally positioned slits.

Acknowledgment

We would like to thank the JR Hokkaido Naebo Workshop, which manufactured the cast iron brake blocks.

References

[1] T. Tsujimura, "Improved Performances of Cast Iron Brake Shoe", QR of RTRI, 35-4, 215-217, 1994.
[2] T. Miyauchi, K. Ohno, T. Tsujimura, J. Nakayama, "Development of a Complex Type Cast Iron Brake Shoe for High Speed Train", QR of RTRI, 39-3, 110-113, 1998.
[3] T. Miyauchi, J. Nakayama, N. Fujiwara, K. Shimoda, S. Nakazawa, S. Fukagai, "Friction and wear performance of nickel and molybdenum-reduction cast iron composite brake blocks including ceramic foams", Wear, 302, 1436-1443, 2013.
[4] Japan patent JP5558019, 2014.